

PACS: 07.77.Ka, 07.85.-m, 61.05.-a, 61.05.C-, 61.72.Lk, 61.72.Mm.

ISSN 1729-4428

I.M. Fodchuk¹, A.R. Kuzmin¹, O.L. Maslyanchuk¹, I.I. Hutsuliak¹, M.S. Solodkyi¹,
Yu.T. Roman¹, M.M. Solovan¹, O.Yo. Gudymenko²

Influence of Dislocation Structure on Electrical and Spectroscopic Properties of MoO_x/p-CdTe/MoO_x Heterostructures

¹Chernivtsi National University, Chernivtsi, Ukraine, i.fodchuk@chnu.edu.ua

²Institute of Semiconductor Physics of NASU, Kyiv, Ukraine

The defect structure of p-CdTe:Cl single crystals and MoO_x/p-CdTe/MoO_x heterostructures were investigated by high-resolution X-wave diffractometry methods. Different models of dislocation systems were used and the dislocation densities were estimated from the Williamson-Hall plot. It is noted that significant deformations of the mismatch in the transition layer negatively affect the current-voltage characteristics of heterostructures.

Keywords: cadmium telluride, defect structure, X-ray multiaxial diffractometry, heterostructures, X- and γ -radiation detectors.

Received 7 October 2021; Accepted 4 March 2022.

Introduction

Semiconductor X- and γ -radiation detectors based on high-resistance CdTe crystals operate at room temperatures and are becoming increasingly common in industrial use. These detectors are as compact as other semiconductor detectors. The energy range from 60 keV to 356 keV is important for their application in medical science and space industry. In addition, they have the desired combination of high braking force, relatively low noise and fast response at room temperature. The mobile heater (THM) method is the most common for growing CdTe crystals. The crystals are doped with chlorine (Cl) to achieve a high resistivity ($\sim 10^8 - 10^{10}$ Ohm·cm). However, the use of Cl as an doping element is associated with performance instability, namely with the polarization of the counting rate and long-term reliability problems [1].

One of the main disadvantages of manufacturing high-efficiency detectors of X- and γ -radiation based on p-CdTe is the problem of reverse ohmic contact. There are no metals that can create ohmic contact with p-CdTe without additional surface treatment [2]. Molybdenum oxide (MoO_x) has found its wide practical application as a material for making high-quality electrical contact with

p-CdTe due to its large operating function (5.2 - 6 eV) [3, 4]. This oxide has a high transparency for visible light and a relatively low electrical resistivity [5-7].

Usually p-CdTe has a complex defective structure, in particular, small-angle boundaries, mosaicity and high dislocation densities [8, 9]. Intrinsic defects that interact with impurities, under certain conditions can create different types of electrically active and inactive complexes, which in turn strongly affect the electronic and mechanical properties of devices made of certain material.

In this paper we investigate the influence of the dislocation structure of p-CdTe:Cl single crystals and MoO_x/p-CdTe/MoO_x heterostructures made on their basis on the electrical and spectroscopic characteristics of X- and γ -radiation detectors.

I. Objects and methods of investigations

The objects of research were two sets of (111) p-CdTe:Cl single crystals of different degrees of structural perfection, grown by the method of mobile heater (AcroRad Co., Ltd, Japan), 5×5×1 mm in size, and MoO_x/p-CdTe/MoO_x heterostructures obtained by the method reactive magnetron sputtering. X-ray studies were

performed on a Panalytical Philips X'Pert PRO diffractometer with $\text{CuK}\alpha_1$ -radiation.

MoO_x films were applied to heated polished p-CdTe single crystal substrates ($5 \times 5 \times 1$ mm in size) by reactive magnetic sputtering at a constant voltage of pure molybdenum target (99.99 % Mo). The process was performed in a universal vacuum unit Leybold-Heraeus, filled with a mixture of argon and oxygen gases.

II. Electric and spectroscopic properties of $\text{MoO}_x/\text{p-cdte}/\text{MoO}_x$ heterostructures

Electrical properties of the $\text{MoO}_x/\text{p-CdTe}/\text{MoO}_x$ heterostructures

The room temperature reverse current-voltage (I - V) characteristics of $\text{MoO}_x/\text{p-CdTe}/\text{MoO}_x$ heterostructures plotted in double logarithmic coordinates show some specific regions (Fig. 1). As seen, at $|V| < 5$ V, the reverse current in the Sample №1 follows square-root dependence ($I \sim V^{0.5}$).

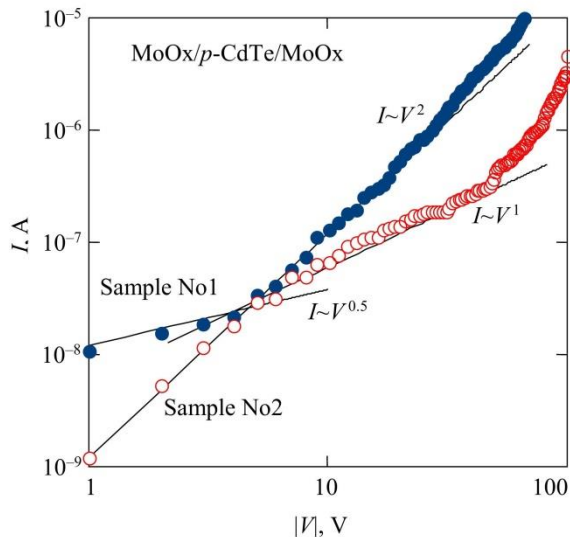


Fig. 1. Room temperature dark reverse I - V characteristic of the $\text{MoO}_x/\text{p-CdTe}/\text{MoO}_x$ heterostructures. Approximations of the linear ($I \sim V^1$), square-root ($I \sim V^{0.5}$), and square-law ($I \sim V^2$) voltage dependences of the current are shown by solid lines.

This is evidence of the fact that the generation charge transport mechanism takes place [10, 11]. At higher voltages the reverse current in the Samples №1 follows quadratic voltage dependence $I \sim V^2$ (Fig. 1), which is typical for the trap-controlled current limited by the negative space charge of electrons in the depleted region of p-CdTe near the MoO_x/CdTe interface, i.e. the Mott-Gurney law is obeyed [12]. It should be noted that the reverse current-voltage dependence in the Sample №2 becomes linear in the voltage range $5 < |V| < 50$ V (Fig. 1). Such a behavior of the I - V characteristic is explained by the fact that the depleted region of the $\text{MoO}_x/\text{p-CdTe}/\text{MoO}_x$ heterostructure occupies almost the entire thickness of the crystal, i.e., this region is limited by the crystal thickness.

Spectroscopic properties of the $\text{MoO}_x/\text{p-CdTe}/\text{MoO}_x$ heterostructures

The $\text{MoO}_x/\text{p-CdTe}/\text{MoO}_x$ detectors are sensitive to X- and γ -ray radiation which are similar to those of our novel Schottky-diode detectors with electrodes made from Ti, Mo, and oxides or nitride of these metals [13], as well as detectors fabricated as Schottky diodes using ion-bombardment of the crystal surfaces before Ni electrode deposition or formed as M-p-n diode structures by laser-induced doping with In. The spectrum of an ^{241}Am (59.5 keV) source measured by the Sample №1 at room temperature are shown in Fig. 2. Worthy of note is the height of the peak of the ^{241}Am source emission spectrum reaches more than 400000 counts.

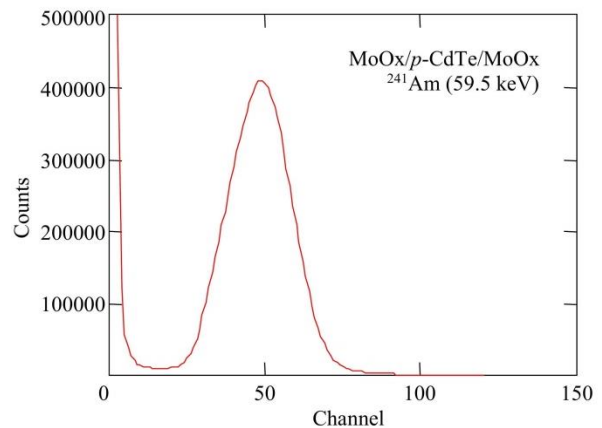


Fig. 2. Room temperature spectrum of an ^{241}Am source obtained by the $\text{MoO}_x/\text{p-CdTe}/\text{MoO}_x$ Schottky-diode detectors at $V = -400$ V.

However, the spectrometric characteristics of the detectors remain quite low. The improvement of detecting properties should be carried out by modification of the condition of contact fabrication and further treatment of the structure to reduce the reverse current.

III. X-ray studies of p-CdTe:Cl single crystals and $\text{MoO}_x/\text{p-CdTe}/\text{MoO}_x$ heterostructures

The defective system of p-CdTe:Cl crystals and $\text{MoO}_x/\text{p-CdTe}/\text{MoO}_x$ heterostructures was investigated by high-resolution X-ray diffractometry. Figure 3 shows the X-ray intensity distributions $I_h(\omega)$ and $I_h(\omega, 2\theta - \omega)$ of p-CdTe:Cl single crystals and $\text{MoO}_x/\text{p-CdTe:Cl}/\text{MoO}_x$ heterostructures obtained for symmetric and asymmetric reflexes. The correspondence between experimental and theoretical values of half-width (W), maximum intensity (I_h^{max}), integral intensity (β) and area under the graph (S) of distributions is one of the criteria for assessment of the degree of crystal structural perfection. The analysis of $I_h(\omega)$ shape shows that sample №1 is quite perfect and

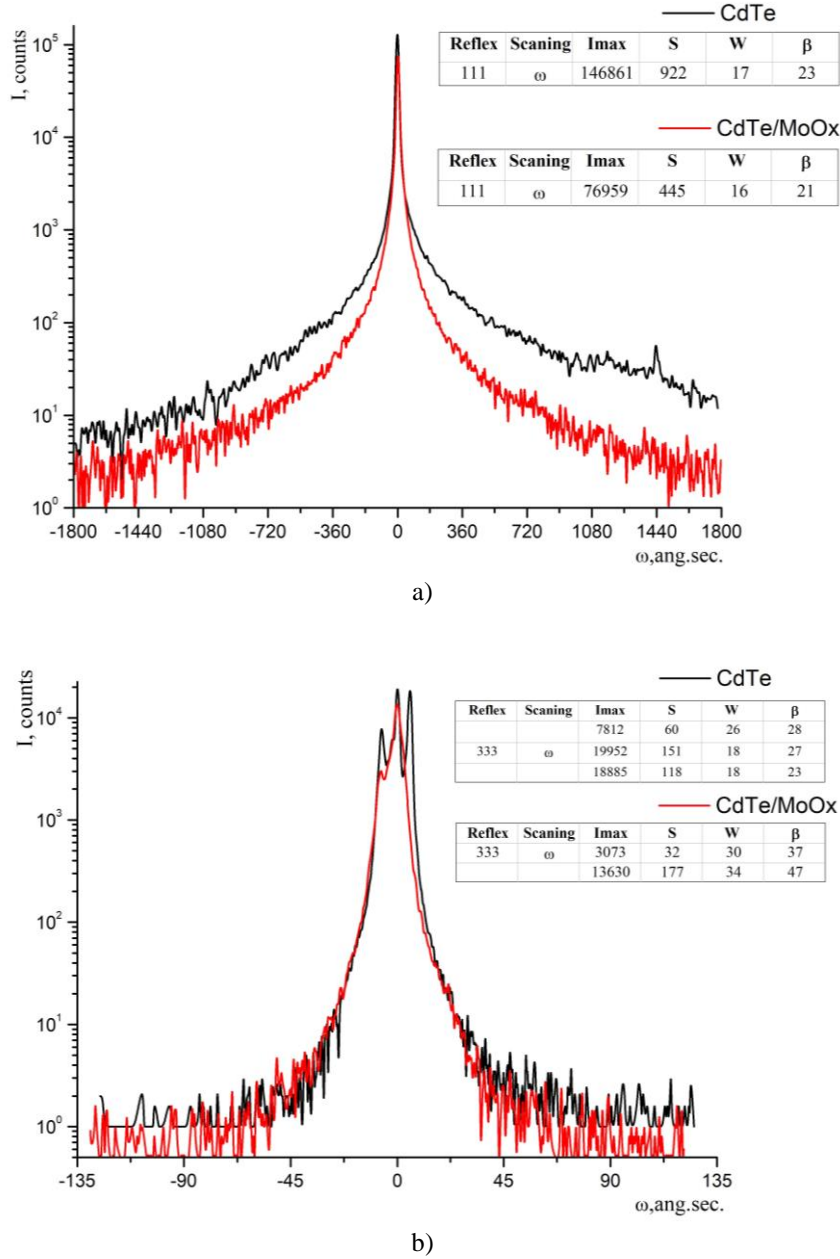


Fig. 3. Rocking curves $I_h(\omega)$, sample №1, reflection (111) (a) and №2, reflection (333) (b), $\text{CuK}_{\alpha 1}$ -radiation.

homogeneous. On the other hand, sample №2 has a developed defective structure. This is evidenced by the presence on $I_h(\omega, 2\theta - \omega)$ distributions of a strong diffuse background and blurring of areas of coherent scattering on $I_h(\omega)$ distributions (Fig. 3).

The most probable dislocation model inherent in CdTe crystals was proposed in paper [14]. According to this theory, two possible systems of dislocations are selected, in particular: a) full 60-degree dislocations with Burgers vectors $\vec{b}_1 = \frac{a}{2} [\bar{1}\bar{1}0]$ and $\vec{b}_2 = \frac{a}{2} [011]$, the lines of which are $(\bar{1}\bar{1}\bar{1})$ in and $(\bar{1}\bar{1}\bar{1})$ planes; b) partial Frank dislocations $\vec{b}_F = \frac{a}{3} \langle 111 \rangle$, the lines of which are oriented in the directions $\langle 0\bar{1}1 \rangle$ and $|\bar{1}01 \rangle$. Such dislocations can also be located in the small-angle boundaries between blocks [14].

Estimation of the density of dislocations N_L in the small-angle boundaries was performed with the relation (1) [15]:

$$N_L = \frac{\Delta\theta}{9|\vec{b}|T}, \quad (1)$$

where $\Delta\theta$ is the angle of disorientation between two blocks, T is the average size of the block, and \vec{b} is the Burgers vector of dislocations typical for the crystal.

Usually, the main contribution to the formation of the coherent component of scattering is made by dislocations. In the case of their chaotic distribution, which occurs in real crystals, the average density of dislocations can be estimated [16]:

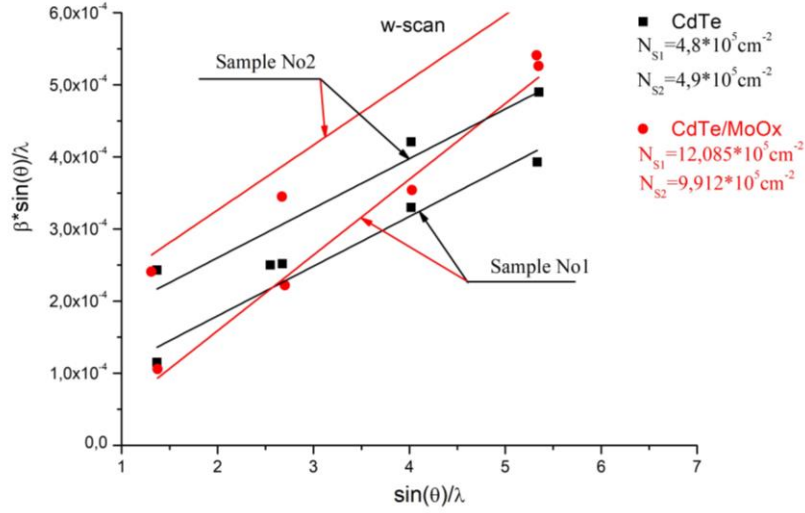


Fig. 4. Williamson-Hall plot for the set of symmetrical (hhh) reflexes and estimation of N_S for samples № 1 and № 2.

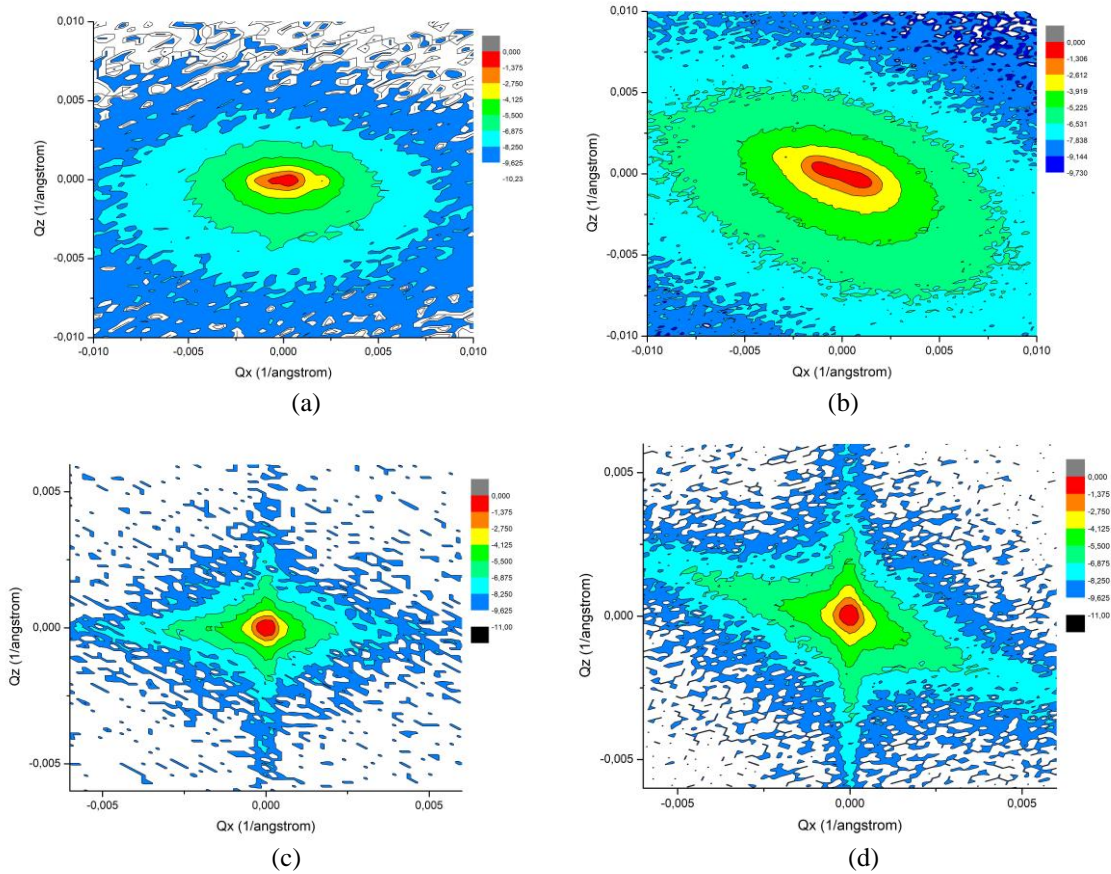


Fig. 5. Reciprocal space maps $I_h(\omega, 2\theta - \omega)$, sample №1, reflection (333) (a,c) and (331) (b,d), $\text{CuK}\alpha_1$ -radiation.

$$N_G = \frac{W_G^2}{9|\vec{b}|^2}, \quad (2)$$

where \vec{b} is the Burgers vector of crystal dislocations.

At the same time Williamson-Hall plot (Fig. 4) [17, 18] was used to calculate possible densities of screw dislocations N_S :

$$N_S = \frac{\alpha^2}{4,35|\vec{b}|^2}, \quad (3)$$

Reciprocal space maps, obtained in symmetric and asymmetric diffraction sets (Fig. 5), provide more complete information about possible changes in the

defective system of the studied samples [19, 20]. The application of the MoOx layer for the sample № 2 made the block structure to become clearer (Fig. 4d), diffuse scattering increased and the region of its distribution expanded. It is due to the fact that in the near-surface layers of the heterostructure there are significant deformations of the mismatch, caused by almost twice the difference in the parameters of the crystal lattices. In particular, for MoOx $a = 3.147 \text{ \AA}$, and for p-CdTe $a = 6.481 \text{ \AA}$. This also indicates an increase in the density of dislocations (Table 1).

Table 1.
Experimental dislocation densities N_G and N_L .

Sample №	reflex	p-CdTe		MoOx/p-CdTe/MoOx	
		N_G , (cm^{-2}) 10^5	N_L , (cm^{-2}) 10^6	N_G , (cm^{-2}) 10^5	N_L , (cm^{-2}) 10^6
1	111	2.6	-	2.2	-
2		17.9	2.1	16.9	3.1
1	333	3.4	-	3.8	-
2		5.8	5.12	14.1	2.4
1	331	1.3	-	5.1	-
2		13.1	5.58	15.7	6.3

Rocking curves (Fig. 3) has specific intensity distribution in coherent scattering region with a strong diffuse background (so called “tails”), indicating about significant structural disturbances in the near-surface layers of heterostructures, possible high dislocation densities and their inhomogeneous volume distribution. Figure 3 shows the intensity distributions for samples № 1 (a) and № 2 (b) before and after application of MoOx layer. The diffuse scattering is more clearly seen on “tails” of $I_h(\omega)$ for symmetrical (333), (444) and asymmetric (331) reflexes (Fig. 3 b). This makes it possible to assess more accurately possible changes in the values of dislocation densities before and after heterostructures creation (Table 1).

Figure 4 shows the values of dislocation densities determined from the Williamson-Hall plot. The dislocation densities for heterostructures increased by an order of magnitude. At present, the dislocation density of more perfect sample № 1 has doubled, while for a more defective sample (№ 2) it has almost tripled (Fig. 4).

The values of dislocation densities N_G and N_L in Table

1 for MoOx/p-CdTe:Cl/MoOx heterostructures indicate their growth.

The initial dislocation density for p-CdTe:Cl samples strongly influences the inverse voltage-current characteristics (Fig. 1). Thus, for heterostructure № 2, the dependence $I(V)$ has a linear shape in contrast to № 1, for which there is a square-root $I(V)$ dependence.

Therefore, significant deformations of the mismatch that occur in the transition layer negatively affect the voltage-current characteristics of heterostructures.

Conclusions

The dislocation density increased by one order of magnitude after application of the MoOx film, which significantly worsened the inverse voltage-current characteristics of the heterostructures. The heterostructure № 2 has atypical linear $I(V)$ dependence, while №1 has typical square-root dependence.

The degree of structural perfection of p-CdTe initial samples should be taken into account first of all to obtain high-quality X- and γ -radiation detectors, as well as the film application technology should be improved, as significant mismatch deformations occur in the transition layer, which also negatively affect the voltage-current characteristics of heterostructures.

Fodchuk I.M. – Ph.D, professor;

Kuzmin A.R. – researcher;

Maslyanchuk O.L. – Ph.D, professor;

Hutsuliak I.I. – Ph.D, assistance professor;

Solodkyi M.S. – Ph.D, assistance professor;

Roman Yu.T. – researcher;

Solovan M.M. – Ph.D, associate professor;

Gudymenko O.Yo. – Ph.D, senior researcher.

- [1] J.F. Butler, F.E Doty, C. Lingren and B. Apotovsky, Presented at the 2nd Topical Meeting on Industrial Radiation and Radioisotope Measurement Applications (Raleigh, September 8-11, 1992); [https://doi.org/10.1016/0168-9002\(96\)00219-7](https://doi.org/10.1016/0168-9002(96)00219-7).
- [2] S. Abbaspour, B. Mahmoudian, and J.P. Islamian, World J Nucl Med. 16(2), 101 (2017); <https://doi.org/10.4103/1450-1147.203079>.
- [3] A. Cola and I. Farella, Applied physics letters 105, 203501 (2014); <https://doi.org/10.1063/1.4902188>.
- [4] O. Maslyanchuk, V. Kulchynsky, M. Solovan, V. Gnatyuk, C. Potiriadis, I. Kaissas, V. Brus, Phys. Stat. Sol. C 14(3–4), 1600232 (2017); <http://dx.doi.org/10.1002/pssc.201600232>.
- [5] O. Maslyanchuk, M. Solovan, V. Brus, P. Maryanchuk, E. Maistruk, I. Fodchuk, V. Gnatyuk, T. Aoki, C. Lambropoulos, K. Potiriadis, IEEE Trans. Nucl. Sci. 65(7), 1365 (2018); <http://dx.doi.org/10.1109/TNS.2018.2838766>.
- [6] L.A. Kosyachenko, O.L. Maslyanchuk, V.M. Sklyarchuk, Semiconductors 39(6), 722 (2005); <https://doi.org/10.1134/1.1944866>.
- [7] O.L. Maslyanchuk, M.M. Solovan, V.V. Brus, V.V. Kulchynsky, P.D. Maryanchuk, I.M. Fodchuk, V.A. Gnatyuk, T. Aoki, C. Potiriadis, Y. Kaissas, IEEE Trans. Nucl. Sci. 64(5), 1168 (2017); <http://dx.doi.org/10.1109/TNS.2017.2694701>.
- [8] O.L. Maslyanchuk, M.M. Solovan, E.V. Maistruk, V.V. Brus, P.D. Maryanchuk, V.A. Gnatyuk, T. Aoki, Proc. SPIE, 10612 (2018); <https://doi.org/10.1117/12.2305085>.
- [9] J. Luschitz, B. Siepchen, J. Schaffner, K. Lakus-Wollny, G. Haindl, A. Klein, W. Jaegermann, Thin Solid Films 517(7), 2125 (2009); <https://doi.org/10.1016/j.tsf.2008.10.075>.

- [10] M.D. Borchа, M.S. Solodkyi, S.V. Balovsyak, V.M. Tkach, I.I. Hutsuliak, A.R. Kuzmin, O.O. Tkach, V.P. Kladko, O.Y. Gudymenko, O.I. Liubchenko, Z. Świątek, *Semiconductor Physics, Quantum Electronics and Optoelectronics* 22(4), 381 (2019); <https://doi.org/10.15407/spqeo22.04.381>.
- [11] V.V. Brus, O.L. Maslyanchuk, M. M. Solovan, P.D. Maryanchuk, I.M. Fodchuk, V.A. Gnatyuk, N.D. Vakhnyak, S.V. Melnychuk, T. Aoki, *Scientific Reports* 9, 1065 (2019); <https://doi.org/10.1038/s41598-018-37637-w>.
- [12] M.A. Lampert, P. Mark, *Current Injection in Solids*, Academic Press (New York, 1970).
- [13] A. Zoul, E. Klier, *Czechoslovak J. Phys. B* 27(7), 789 (1977); <https://doi.org/10.1007/BF01589320>.
- [14] I. Fodchuk, A. Kuzmin, I. Hutsuliak, M. Solodkyi, V. Dovganyuk, O. Maslyanchuk, Yu. Roman, R. Zaplitnyy, O. Gudymenko, V. Kladko, V. Molodkin, V. Lizunov, *Proc. SPIE* 113691H (2020); <https://doi.org/10.1117/12.2553970>.
- [15] X. Chut, B.K. Tanner, *Semicond. Sci. Tech.* 2, 765 (1987); <https://doi.org/10.1088/0268-1242/2/12/002>.
- [16] P.B. Hirt, *Mosaic structure* (Metallurgy, Moscow, 1960).
- [17] E. Schafner, M. Zehetbauer, and T. Ungar, *Materials Science and Engineering*. 319-321, 220 (2001); [https://doi.org/10.1016/S0921-5093\(01\)00979-0](https://doi.org/10.1016/S0921-5093(01)00979-0).
- [18] E. Metzger, R. Hopler, and E. Born, *Philosophical Magazine*. 77(4), 1013 (1998); <https://doi.org/10.1080/01418619808221225>.
- [19] I.M. Fodchuk, V.V. Dovganiuk, I.I. Gutsuliak, I.P. Yaremiiy, A.Y. Bonchuk, G.V. Savytsky, I.M. Syvorotka, O.G. Skakunova, *Metallofizika i Noveishie Tekhnologii* 35(9), 1209 (2013).
- [20] M.D. Borchа, M.S. Solodkyi, S.V. Balovsyak, V.M. Tkach, I.I. Hutsuliak, A.R. Kuzmin, O.O. Tkach, V.P. Kladko, O.Y. Gudymenko, O.I. Liubchenko, Z. Świątek, *Semiconductor Physics, Quantum Electronics and Optoelectronics* 22(4), 381 (2019); <https://doi.org/10.15407/spqeo22.04.381>.

I.M. Фодчук¹, А.Р. Кузьмін¹, О.Л. Масляничук¹, І.І. Гуцуляк¹, М.С. Солодкий¹,
Ю.Т. Роман¹, М.М. Солован¹, О.Й. Гудименко²

Вплив дислокаційної структури на електричні та спектроскопічні властивості гетероструктур $\text{MoO}_x/\text{p-CdTe}/\text{MoO}_x$

¹Чернівецький національний університет, Чернівці, Україна, i.fodchuk@chnu.edu.ua

²Інститут фізики напівпровідників НАНУ, Київ, Україна

Методами високороздільної Х-хвильової дифрактометрії досліджена дефектна структура монокристалів р-CdTe:Cl та на їх основі гетероструктур $\text{MoO}_x/\text{p-CdTe}/\text{MoO}_x$. Апробовано різні моделі дислокаційних систем, за якими із побудови Вільямсона-Холла оцінено густини дислокацій. Відзначено, що значні деформації невідповідності в перехідному шарі негативно впливають на вольт-амперні характеристики гетероструктур.

Ключові слова: телурид кадмію, дефектна структура, високороздільна Х-променева дифрактометрія, гетероструктури, детектори Х- та γ - випромінювання.